

An AODV Routing Algorithm Based on Optimal Search Region and Energy-Aware

Haowei Ma, Zhijun Tang*, Shanshan Dong

School of Information and Electrical Engineering, Hunan University of Science and Technology, Xiangtan 411201, China

*Corresponding author: Zhijun Tang

Abstract: To address the issues of high control overhead caused by global route re-establishment during link fractures, network performance degradation due to energy imbalance, and in-sufficient link stability resulting from the lack of energy awareness in traditional flooding mechanisms in the Ad-hoc On-Demand Distance Vector (AODV) routing protocol, this paper proposes an enhanced SE-AODV routing algorithm (An AODV Routing Algorithm Based on Optimal Search Region and Energy-Aware) based on localized repair and energy-sensitive selection mechanisms. When a link fracture occurs due to node energy exhaustion or movement beyond the communication range, the detecting node sends a repair request to the upstream vertex node based on hop count, physical distance, and residual energy of neighboring nodes. The vertex node initiates a localized repair process, determining the optimal search region by calculating the sector angle θ through multi-objective weighted optimization. This θ -constrained flooding region reduces redundant control overhead. Subsequently, regional validation is performed for candidate next-hop nodes, prioritizing those with higher residual energy to avoid premature energy depletion in low-energy nodes and enhance link stability. Simulation results demonstrate significant improvements in three key metrics: average end-to-end delay, packet delivery rate, and routing control overhead.

Keywords: AODV; link repair; residual energy; flooding restriction

Date of Submission: 01-11-2025 Date of acceptance:

10-11-2025

I. Introduction

Mobile adhoc networks (MANETs) require no fixed infrastructure, representing a multi-hop wireless self-organizing network. MANETs have now gained widespread applications ^[1]. However, due to bandwidth resource constraints and limited node energy in wireless networks, routing protocols should be designed to reduce their consumption of network bandwidth resources and energy expenditure while meeting application requirements, enhancing protocol efficiency and network throughput.

Based on different scenarios, wireless routing protocols mainly fall into two paradigms: table-driven routing (proactive routing) and on-demand driven routing (reactive routing), with their core distinctions reflected in working mechanisms, resource consumption, and applicable scenarios. In table-driven routing, nodes proactively maintain network-wide routing tables, updating routing information in real-time through periodic broadcasts or triggered updates upon topology changes. Route discovery and maintenance are continuously performed, with all nodes storing complete routing information regardless of current communication needs. Examples include DSDV (Destination Sequenced Distance Vector Routing)^[2-5] and OLSR (Optimized Link State Routing)^[6-10]. On-demand driven routing triggers route discovery only when data transmission is required. The source node dynamically discovers paths by broadcasting Route Requests (RREQs), with intermediate nodes potentially caching partial route information to optimize subsequent requests. Route maintenance is performed only when communication links are interrupted. Examples include DSR (Dynamic Source Routing)^[11-12] and AODV (Ad-hoc On-Demand Distance Vector)^[13-16]. On-demand driven routing suits networks with strong dynamic performance and frequent node mobility such as MANETs. It features low control overhead, triggers route discovery only when needed, conserves bandwidth and node storage resources, and extends network lifetime.

| IJMER | ISSN: 2249–6645 | Nov.-Dec.2025| 1 |

www.ijmer.com | Vol. 15 | Iss. 6 |

II. Related Works

The AODV routing protocol is a classic on-demand routing protocol, with its operation centered around two main phases: route discovery and route maintenance, reducing network overhead through dynamic routing table management. Its trigger condition occurs when a source node needs to send data to a destination node but lacks a valid path in its local routing table, initiating the route discovery process. If no destination node exists, the source node floods^[17] RREQs (Route Requests). Intermediate nodes decide whether to forward based on whether they receive the RREQ for the first time, establishing temporary routes through reverse path setup. Upon receiving the first RREQ, the destination node unicasts RREPs back to the source node along the reverse path via intermediate nodes, successfully establishing the routing path.

Generally, the AODV protocol employs overly simplistic routing criteria, using hop count as the sole path selection standard while ignoring factors like node energy, link quality, and congestion level. Regarding flood control and redundant broadcasting, route discovery relies on broadcast flooding mechanisms, which can easily trigger broadcast storms in high-density scenarios. Routing decisions fail to consider energy issues, causing premature failure of low-energy nodes.

In recent years, many scholars have improved the AODV routing protocol from various aspects. Reference[18] optimized AODV to address frequent route interruptions caused by ignoring node energy status, selecting nodes with higher energy and stronger signal strength during route discovery to extend network lifetime. Reference[19] proposed a Max-Min energy algorithm to calculate node residual energy, but computing and comparing residual energy across the entire network requires frequent control message exchanges, potentially increasing channel occupancy and node energy consumption, leading to higher routing control overhead. Reference[20] dynamically calculated forwarding probabilities based on neighbor node count and adopted cross-layer design to select routing paths according to link weights. Reference[21] divided functions into three regions—edge, corner, and center—using piecewise functions, then calculated node degrees in these regions. It employed a static game forwarding strategy to forward route request packets, estimating node counts through node degrees to reduce redundancy in route broadcasting and improve broadcast efficiency. Reference[22] expressed congestion levels and residual energy per path segment as hop costs, classifying them into different levels based on predefined thresholds. The path with the lowest comprehensive hop count was selected as optimal, effectively reducing network congestion. Reference[23] proposed two optimized protocols-E-AODV and RE-AODV-to address intermediate nodes discarding RREP packets due to insufficient energy when destination nodes reply with RREP messages. These introduced energy thresholds and "minimum residual energy" mechanisms: E-AODV prevents node battery depletion to enhance network performance, while RE-AODV optimizes through RREP message broadcasting and energy threshold filtering. However, broadcasting itself increases channel contention and may cause control packet flooding in high-density scenarios, exacerbating channel congestion. Overall, improving AODV involves:Designing multi-dimensional routing criteria combining hop count, link quality, congestion level, etc. Rather than relying solely on hop count; Introducing energy balancing and conservation mechanisms by setting energy thresholds or hierarchical strategies to prioritize high-energy nodes and improve network performance; Incorporating flood limiting functions to reduce redundant broadcasts.

Addressing the shortcomings of existing AODV improvements, this paper proposes an enhanced AODV algorithm based on optimal search area and energy sensitivity. When certain paths between source and destination nodes break, instead of global flooding for rediscovery, the algorithm initiates from the predecessor node of the broken link. Based on its position relative to the broken node and surrounding nodes' energy sensitivity levels, an optimal search area is formed. Within this area, high-energy nodes are selected to avoid low-energy nodes that degrade link quality.

III. SE-AODV Algorithm Design

3.1 Scenario Description

The traditional AODV routing protocol employs global flooding^[24] to disseminate RREQ messages and selects the minimum hop count as the propagation path. It can be argued that nodes selected for broken link repair may not be optimal solutions, thereby increasing network control overhead. This paper designs an optimal search area to constrain flooding propagation.

In an ad hoc network, when source node S needs to establish a route to destination node D but lacks such route entry in its routing table, it must initiate a route discovery process^{[25-27].} This begins with broadcasting Route Request packets to its neighboring nodes. Intermediate node M decides whether to forward based on whether it receives the RREQ for the first time; if not, it discards it. Other nodes repeat this process until the

| IJMER | ISSN: 2249–6645 | www.ijmer.com | Vol. 15 | Iss. 6 |

Nov.-Dec.2025| 2 |

message reaches destination node D. Upon receiving the message, node D replies to source node S with an RREP (Route Reply) along the reverse path, successfully establishing a complete route [28-29].

Compared to other protocols, AODV initiates route discovery only when necessary ("on-demand" operation), which benefits network performance. However, due to frequent node mobility in adhoc networks, route validity periods are short. When a node moves beyond communication range and cannot forward packets, the route fails, indicating link breakage. If the source node wishes to continue propagating RREQ messages to establish routes, it must repair the broken link, which is shown in Figure 1.

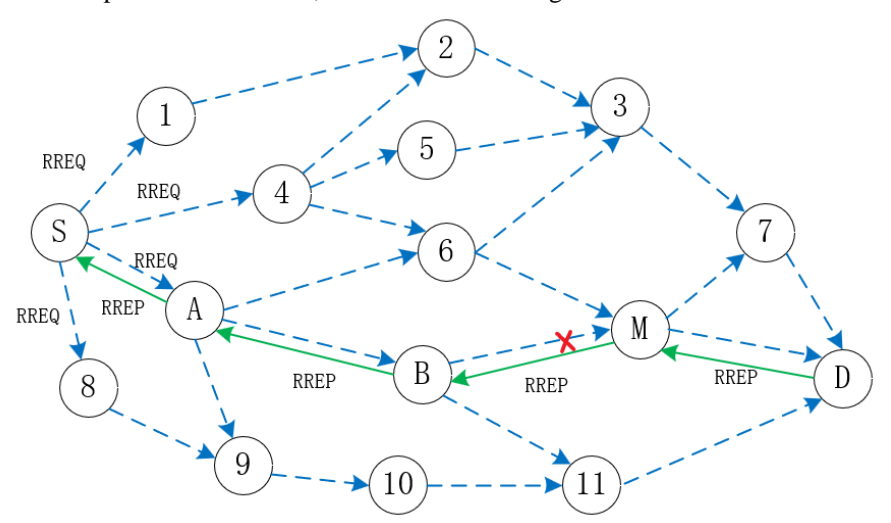


Figure 1 Communication process of the AODV protocol

3.2 Establishment of Optimal Search Area

energy_ratio

α, β, γ

This paper defines the upstream node of a broken link as the Vertex. The next-hop node discovered through the optimal search area initiated from this Vertex is termed the Advantage Point. In an AODV path, when node M fails to propagate data to the next hop due to energy depletion or moving beyond node B's communication range, causing link breakage, node B sends an RRMR (Route Repair Mistake Report) to upstream node A. This report contains the hop count, position, and distance to destination node D. Upon receiving the RRMR, Vertex A acquires the hop count, position, and distance to node D, initiating link reconstruction. During reconstruction, only neighboring nodes participate in link repair through local flooding to find alternative paths, without affecting other nodes' ongoing data transmission. After receiving the RRMR, Vertex A defines the included angle θ through three dimensions: path hop count, actual physical distance, and node energy.

$$\theta = \left[\alpha \frac{hops_md}{hops_am + hops_md} + \beta (1 - \frac{dist_am/r}{hops_am}) + \gamma \cdot energy_ratio \right] \times \theta_{max}$$
 (1)

Table 1 Variables Involved and Their Physical Meanings.		
Variable Name	Definition	
θ	Included angle formed with Vertex and Destination Node as axis	
$ heta_{ m max}$	Initial value: 90°	
hops_md	Hop count from Broken Node (M) to Destination Node (D)	
hops_am	Hop count from Vertex (A) to Broken Node (M)	
dist_am	Physical distance from Vertex (A) to Broken Node (M)	

The optimal search area is a sector-shaped region based on θ , which is shown as in Figure 2.

| IJMER | ISSN: 2249–6645 | Nov.-Dec.2025|3|

Node communication radius

Node residual energy ratio

Weight coefficients satisfying $\alpha + \beta + \gamma = 1$

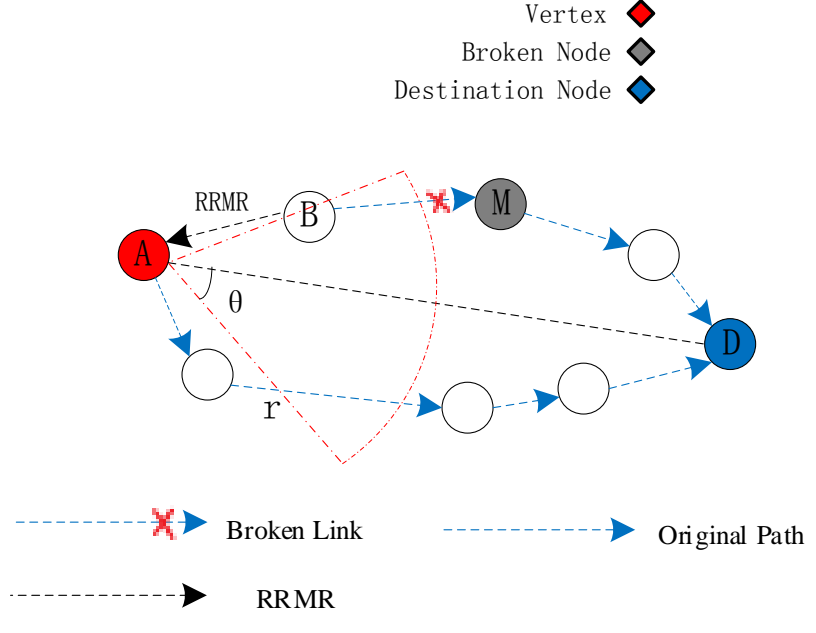


Figure 2 Calculation of the θ angle

Broadcasting route requests within the area prioritizes high-energy nodes as next hops, effectively reducing flooding control overhead. The formula comprises three components. Part 1:

$$P1 = \frac{hops_md}{hops_am + hops_md}$$
 (2)

Where P1measures the path proportion from the broken node to the destination. If the destination is far from the broken node (large hops_md), this term increases, expanding the included angle θ and enlarging the optimal search area; conversely, θ contracts, reducing the search area. Part 2

$$P2 = \left(1 - \frac{\text{hops} _\text{am} / r}{\text{hops} _\text{am}}\right) \tag{3}$$

Where P2 combines physical distance and hop count to adjust the detection direction, where r denotes the node communication radius. The distance from Vertex A to broken node M is dist_am:

dist
$$_$$
 am $= \sqrt{(M_y - A_y)^2 + (M_x - A_x)^2}$ (4)

Where $dist_am/r$ represents the normalized distance from Vertex to broken node. If the actual distance approaches r and hops_am is large, θ expands to increase the optimal search area; otherwise, θ contracts, reducing the area. Traditional AODV always selects paths based solely on hop count while ignoring node energy. Selecting low-energy nodes within the θ -defined area for data propagation would deplete node energy, compromising link stability. Therefore, when calculating θ , an energy sensitivity factor $energy_ratio$ positively correlated with residual energy is added alongside distance and hop count. This ensures nodes with higher residual energy increase θ , making them more likely to be included in the search area, effectively extending network lifetime and optimizing performance. The node energy consumption formula is defined as:

$$\begin{cases} E_{Si} = \eta_1 E_{elec} + \eta_1 \varepsilon L^2 \\ E_{Ri} = \eta_2 E_{elec} \end{cases}$$
 (5)

Where $E_{\rm Si}$ is the energy consumed by node i for transmitting data packets, $E_{\rm Ri}$ is the energy consumed by node i for receiving data packets, η_1 and η_2 are efficiency coefficients for transmission and reception. ε is generally a constant, $\varepsilon = 10 \, pJ \, / \, (bit.m^{-2})$. $E_{\rm elec}$ is the energy consumed per unit data for transmission/reception, $E_{\rm elec} = 50 \, nJ \, / \, bit$. L is the distance between neighboring nodes. The residual energy $E_{\rm i}$ of a node is calculated from its initial energy, $E_i = E_0 - E_{\rm Si} - E_{\rm Ri}$. Based on the above information, the residual energy ratio of node i can be derived:

| IJMER | ISSN: 2249–6645 | v Nov.-Dec.2025|4|

$$energy_ratio = \frac{E_i}{E_0}$$
 (6)

In an ad hoc network, the initial energy of any node is E₀. A higher residual energy ratio value indicates greater remaining energy in nodes available for communication. When a node's residual energy ratio reaches 0, it signifies energy exhaustion, rendering it ineligible as a next hop for data propagation. The entire path passing through this node breaks and fails, initiating self-repair of the broken path. α , β , and γ are dynamic weighting coefficients adjusted based on network density, energy distribution, etc. Among these, y represents the weight for residual energy, regulating the priority of including high-energy nodes within the area. α denotes the weight for hop count proportion, reflecting the hop count ratio from the broken node to the destination. In high-density networks where hop count information carries greater weight, the algorithm prioritizes hop proportion by increasing a. B represents the weight for distance proportion, reflecting the normalized value of average distance per hop. In sparse low-density networks where physical distance critically impacts path stability, β can be increased.

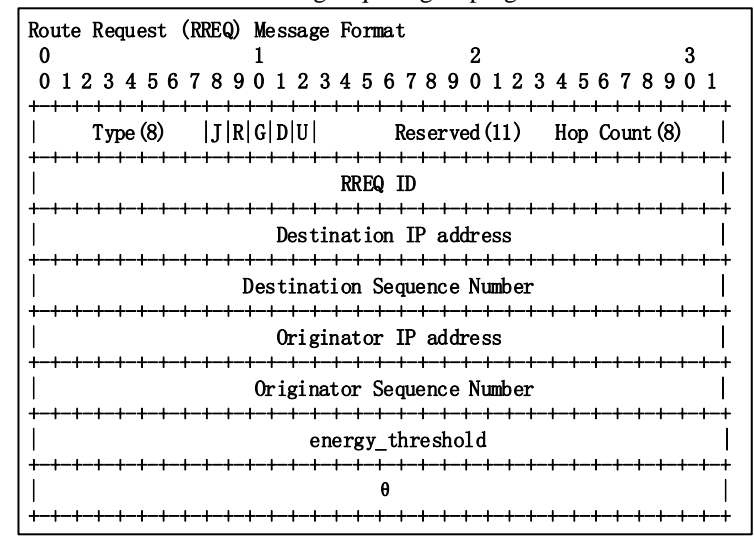


Table 2 Routing request grouping structure

The original AODV protocol's RREQ packets lack fields for energy thresholds and included angle θ information, preventing Advantage Point screening within bounded areas. Consequently, the RREQ packet format is modified to add fields related to energy thresholds and included angle θ . The RREQ packet format for SE-AODV is shown in Table 2.

Continuingrouting participation when a node's residual energy nears exhaustion significantly increases link failure rates, causing disconnections. To prevent selecting low-energy nodes within bounded areas, the energy_threshold (hereafter referred to as E_t) is set to $0.4^{[30]}$. When anode receives an RREQ message, it checks its residual energy ratio against E₁. If energy ratio <E₁, the node does not forward the RREQ. When a link breaks in an active route and the distance between the upstream node at the breakpoint and the destination does not exceed themaximum repair length (MAX_REPAIR_TTL), this upstream node may locally repair the broken link. The upstream node then:1) Increment the destination's sequence number by 1. 2) Broadcasts RREQ packet to the destination.3) Sets the TTL in the RREQ packet to:MAX(MIN_REPAIR_TTL, Latest 0.5×#hops)+LOCAL_ADD_TTL.Where MIN_PEPAIR_TTL: known hop destination.#hops:Hop count to the source node of the currently undeliverable packet.Local repair operations are typically invisible to the source node and require TTL\(\ge MIN_REPAIR_TTL + LOCAL_ADD_TTL\). The node initiating local repair then waits for one route discovery period to receive RREP responses to the RREO.

| IJMER | ISSN: 2249–6645 | | Vol. 15 | Iss. 6 | www.ijmer.com

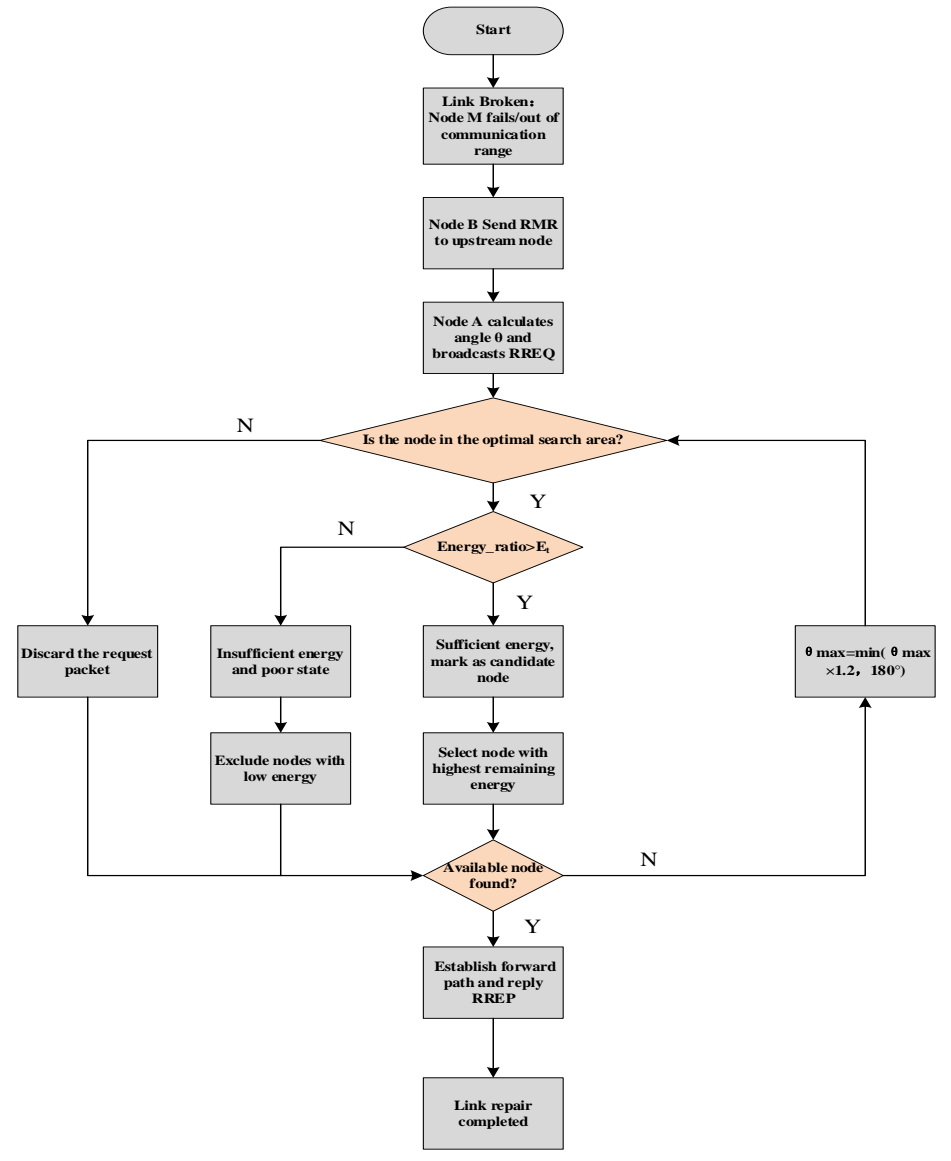


Figure 3 Link repair flowchart

The RREP structure of the SE-AODV routing algorithm is consistent with the AODV route reply. The RREP structure of the SE-AODV routing algorithm is shown in Table 3.

Table 3 Route reply grouping structure

IV. Broken Link Repair Process

The detailed flowchart of the SE-AODV algorithm is shown in Figure 3.Broken link repair process is described as follows:

- 1) When node M causes link breakage due to energy depletion or moving beyond node B's communication range, node B proactively sends an RRMR to upstream node A.
- 2) Upon receiving the RRMR, node A initiates link repair, calculates the included angle θ using formula (1), adds it to the RREQ packet, and broadcasts route requests containing energy threshold and included angle θ within the optimal search area to discover Advantage Points. Upon receiving node A's broadcasted route request, nodes F and G first determine whether they reside within the θ -defined area. They calculate angles \angle

FAD and \angle GAD using the angle formula (see formula (10)), hereafter denoted as α_f and α_g . If $\alpha_f \le \theta$ and $\alpha_g \le \theta$, nodes F and G are within the optimal search area and continue broadcasting the route request (proceed to 3); otherwise, they discard it (proceed to 4).

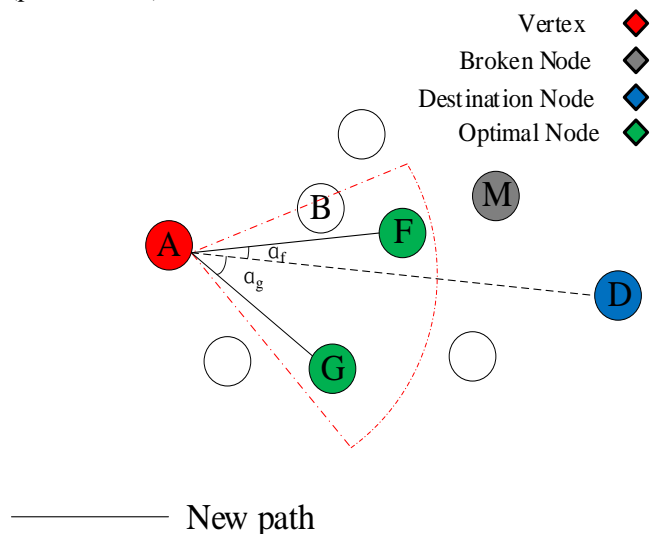


Figure 4 Search for optimal nodes within the optimal search area

$$\overrightarrow{AF} = (x_f - x_a, y_f - y_a) (7)$$

$$\overrightarrow{AD} = (x_d - x_a, y_d - y_a)_{(8)}$$

$$\cos \theta = \frac{\overrightarrow{AF} \cdot \overrightarrow{AD}}{|AF| \cdot |AD|} = \frac{(x_f - x_a)(x_d - x_a) + (y_f - y_a)(y_d - y_a)}{\sqrt{(x_f - x_a)^2 + (y_f - y_a)^2 \cdot (x_d - x_a)^2 + (y_d - y_a)^2}} (9)$$

$$\theta = \arccos \frac{(x_f - x_a)(x_d - x_a) + (y_f - y_a)(y_d - y_a)}{\sqrt{(x_f - x_a)^2 + (y_f - y_a)^2} \cdot \sqrt{(x_d - x_a)^2 + (y_d - y_a)^2}} (10)$$

3) Nodes within the optimal search area undergo energy screening:

If energy_ratio<E_t: The node is discarded due to high channel congestion and energy consumption. Selecting it risks premature energy exhaustion and link breakage.

If energy_ratio \geq E_t: The node is prioritized based on residual energy. The highest-energy node is selected as it maintains idle channel occupancy and optimal operational status for reliable data transmission/reception.

4) If no qualified nodes exist in the search area, θ_{max} dynamically expands:

 $\theta_{\text{max}} = \min(\theta_{\text{max}} \times 1.2,180^{\circ}) (11)$

and updates the RREQ, and returns to step 2) for re-evaluation to prevent repair failure.

5) Subsequent nodes repeat the above steps until the destination node receives the route request and replies with RREP to establish the forward path.

Pseudocode of the SE-AODV Algorithm is shown as Table 4.

Table 4Pseudocode of the SE-AODV Algorithm.

```
Optimal Search Region and Energy-Aware Selection AODV Routing Algorithm
if (current link to next-hop node is broken)
Send RRMR to upstream node
Upstream node calculates search angle \theta
Broadcast RREQ with (\theta, E_t) in sector area
end if
if (node outside \theta angular range)
 Drop RREO
 \theta_{max} = \theta_{max} \times 1.2
if (\theta_{max} > 180^{\circ})
 \theta_{max} = 180^{\circ}
Exit
else
 Proceed to Energy Validation
end if
energy_ratio = residual_energy / initial_energy
if (energy\_ratio < E_t) then
Mark as congested node
Drop RREQ
else
Add to candidate_list
Sort candidate_list by energy DESC
 while (candidate list is empty) do
    \theta_{max} = \theta_{max} \times 1.2
    if (\theta_{max} > 180^{\circ})
       \theta_{max} = 180^{\circ}
    end if
      Re-broadcast RREQ with new \theta
     Receive new candidates
    end while
     Repeat Steps 2-5 until destination reached
     Destination sends RREP through reverse path
     Update routing table with new path metrics
    if (route repair fails after 3 attempts)
        Initiate full route discovery
    end if
End
```

V. Simulation and Results

5.1 Simulation Parameter Settings

The experiment uses MATLAB software to simulate and analyze the improved AODV algorithm proposed in this paper. The protocol is compared with classic AODV, AODV-C, and AODV-E protocols. Adopting theRand Way-point mobility model^[31], simulations are conducted based on three metrics: average end-to-end delay, packet delivery ratio, and routing control overhead. The simulation duration is 500 seconds. Simulation parameters are shown in Table 5.

Table 5Network parameter values for different environmental parameters

Simulation Parameter	Value
Simulation Time/s	500

| IJMER | ISSN: 2249–6645 | www.ijmer.com | Vol. 15 | Iss. 6 |

Nov.-Dec.2025| 8 |

Number of Nodes	100
Scenario Size /m	1000×1000
Maximum Node Speed/(m·s ⁻¹)	10
Initial Node Energy/J	100
Node Communication Radius/m	240
Packet Size/b	512
Maximum Packet Transmission Rate/s	10
Mobility Model	Rand Way-point
Node Energy Threshold/J	0.4

5.2Performance Metrics

In general, average end-to-end delay, packet delivery ratio and routing control overheaddirectly and comprehensively reflect the core performance, efficiency, and scalability of a routing protocol. Analysis of their performance trade-offs is the most authoritative method for comparing various routing protocols by using these three metrics.

(1) Average End-to-End Delay

Average end-to-end delay refers to the average time required for a data packet to be transmitted from one node and received by the next node. Low delay is a crucial manifestation of a protocol's efficiency and adaptability. The calculation method is shown in Formula (12).

$$Avdelay = \frac{1}{N} \sum_{i=0}^{N} (T_{end}(i) - T_{start}(i))$$
(12)

(2) Packet Delivery Ratio (PDR)

Packet Delivery Ratio refers to the ratio of the number of data packets successfully transmitted to the destination node to the total number of packets sent by the source node. It directly measures the protocol's ability to accomplish data transmission in specific network environments. A higher PDR indicates better routing effectiveness and more reliable data transmission. The calculation method is shown in Formula (13).

$$PDR = \frac{P_R}{P_S} \times 100\% \tag{13}$$

(3) Routing Control Overhead

Routing Control Overhead refers to the proportion of control messages (RREQ, RREP, RERR, HELLO) consumed by the protocol to maintain routes relative to the total traffic. It reflects the protocol's scalability. Lower routing overhead indicates reduced resource consumption required for route selection within the network. The calculation formula is shown in (14).

$$N_{load} = \frac{P_C}{P_D} \tag{14}$$

5.3 Simulation Results

As shown in Figure 5, the network's average delay generally exhibits an upward trend due to increasing packet transmission rates causing network congestion. Queueing for data transmission further exacerbates network load. The original AODV protocol demonstrates the poorest delay control performance. AODV-E prioritizes high-energy nodes, showing slightly lower delay than AODV-C at low transmission rates. However, as transmission rates increase, its frequent energy monitoring causes dramatic delay surges. AODV-C maintains lower delays than both AODV and AODV-E, though flood-limiting mechanisms may ignore certain paths leading to minor delay increases at higher rates. The proposed SE-AODV protocol performs optimally, reducing average delay by approximately 64.96% compared to traditional AODV, 39.95% versus AODV-E, and 26.90% versus AODV-C, demonstrating significant delay reduction.

Figure 6 indicates that initial low transmission rates and light network load maintain optimal performance with infrequent route discovery. As transmission rates increase, packet delivery ratios decline due to excessive packets intensifying channel contention and collisions. Intermediate nodes handling multiple packets may discard overloaded traffic, reducing delivery rates. While AODV-E avoids low-energy nodes to minimize failure-induced packet loss, its energy monitoring overhead degrades performance at extreme rates. AODV-C limits flooding but prioritizes minimum hops, selecting unstable low-energy links especially noticeable at high rates. SE-AODV comprehensively selects energy-sufficient stable links, achieving the

highest delivery ratio with minimal decline during rate increases—improving delivery by approximately 22.7% over traditional AODV, and 18.32% and 19.2% over AODV-C and AODV-E respectively.

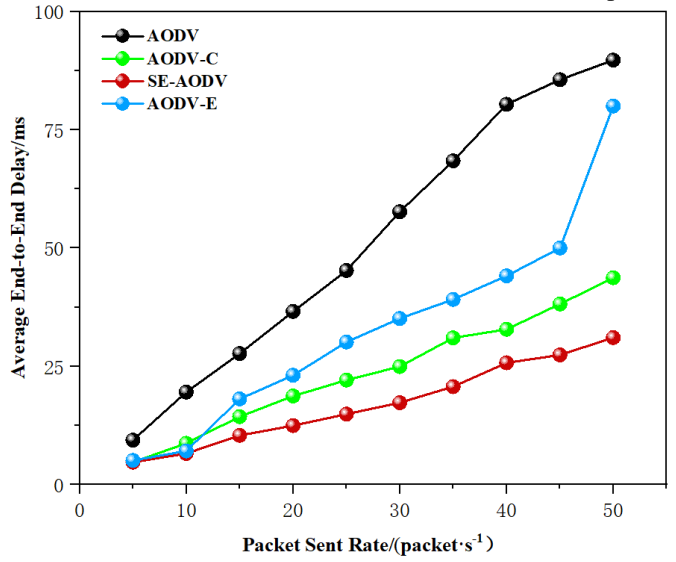


Figure 5 The impact of packet sent rate on average end-to-end delay

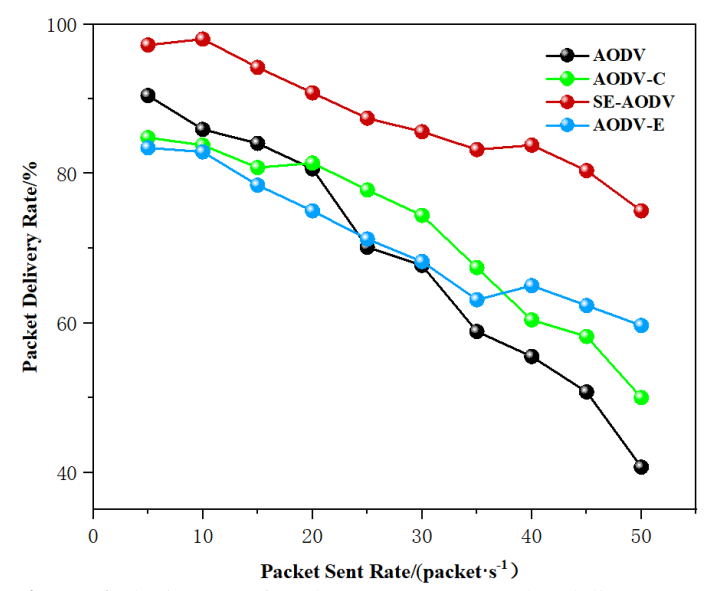


Figure 6 The impact of packet sent rate on packet delivery rate

Figure 7 reveals that as transmission rates rise, SE-AODV and AODV-C exhibit significantly lower routing overhead than AODV and AODV-E. This occurs because AODV and AODV-E employ flood-based forwarding in medium-high rate regions, generating excessive packet transmissions/receptions that increase control overhead. AODV-C's flood restriction reduces route request broadcasts, resulting in slower overhead growth during rate increases. SE-AODV avoids network-wide flooding through optimal search areas, forwarding via highest residual-energy-ratio nodes while filtering unqualified nodes to reduce packet transmissions. Its control overhead decreases by approximately 93.55% versus traditional AODV, and 81.08% and 83.44% versus AODV-C and AODV-E respectively, demonstrating substantial congestion reduction through overhead optimization.

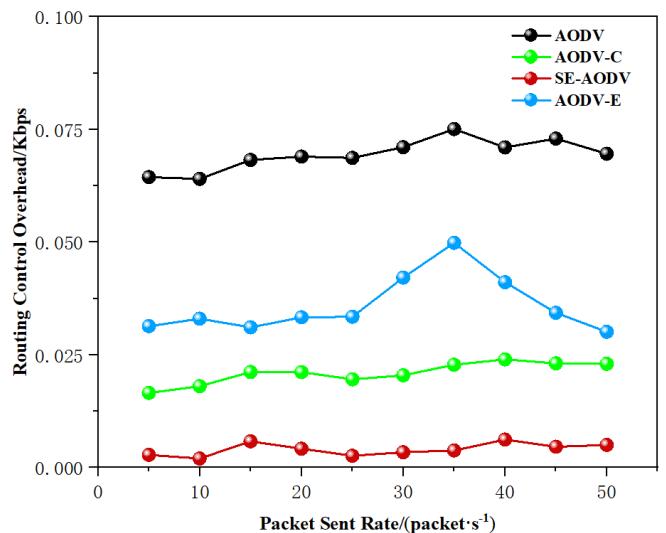


Figure 7 The impact of packet sent rate on routing control overhead

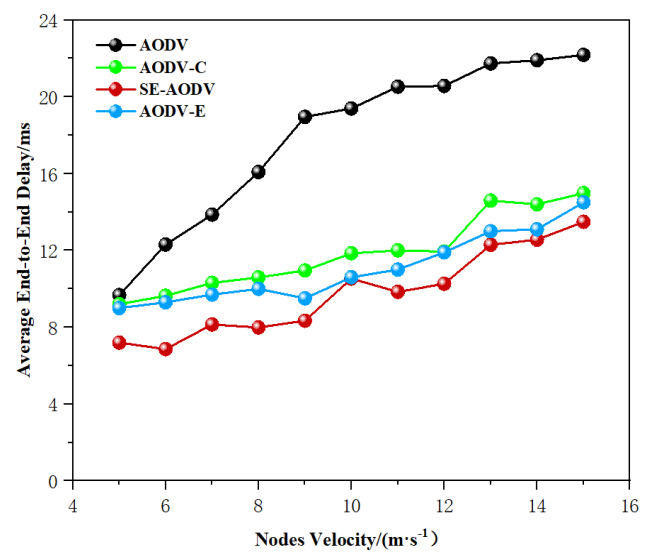


Figure 8 The impact of nodes velocity on average end-to-end delay

Figures 8-10 present simulation results for average end-to-end delay, packet delivery ratio, and routing control overhead under varying node mobility speeds. Figure 8shows that as node speed increases, all four protocols exhibit rising average delay. AODV demonstrates significantly higher transmission delay that escalates markedly with speed due to accelerated topology changes, which increase route interruption probability. Each interruption requires new route discovery, introducing additional latency and higher control overhead. AODV-C reduces route discovery time through flood restriction, maintaining lower delay. However, as mobility increases, faster topology changes cause more link breaks and rerouting, resulting in moderate delay increases. AODV-E prioritizes high-energy nodes to avoid premature exhaustion, but potentially selects longer detour paths, exacerbating delay at high speeds. The proposed SE-AODV combines flood restriction and energy-aware selection, demonstrating strong performance in high-mobility scenarios. It reduces delay by approximately 49.26% compared to traditional AODV, and by 22.64% and 18.92% versus AODV-C and AODV-E respectively.

| IJMER | ISSN: 2249–6645 | www.ijmer.com Nov.-Dec.2025| 11 |

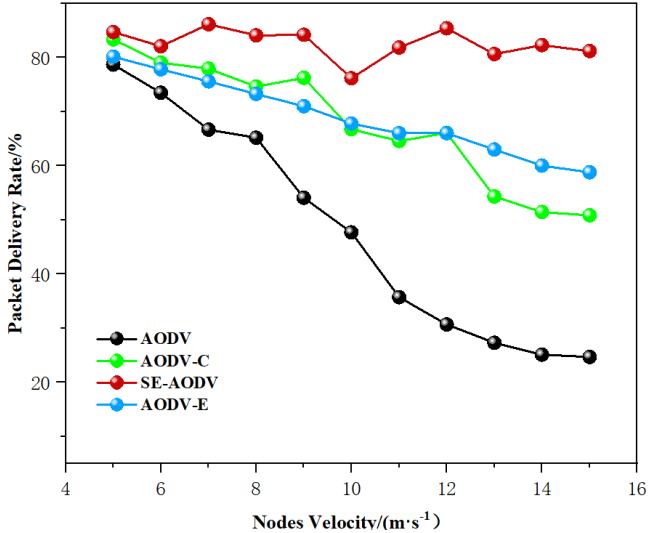


Figure 9 The impact of nodes velocity on packet delivery rate

Figure 9 reveals an inverse correlation between node speed and packet delivery ratio. AODV-E reduces packet loss from node failures by avoiding low-energy nodes, achieving higher delivery than AODV. However, path detours cause slight degradation at high speeds. AODV-C's flood restriction may select suboptimal paths, yielding lower delivery than SE-AODV. SE-AODV integrates energy awareness and flood restriction, maintaining optimal and stable delivery even under high mobility. It minimizes delivery degradation, improving delivery by approximately 32.53% over AODV, and by 7.1% and 10.27% over AODV-C and AODV-E respectively.

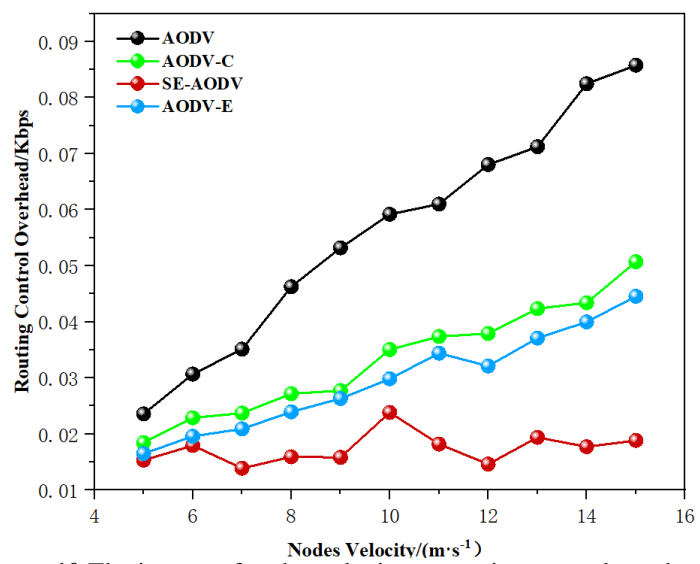


Figure 10 The impact of nodes velocity on routing control overhead

In Figure 10, control overhead rises with increasing speed across all protocols. AODV incurs the highest overhead due to global flooding. AODV-E requires frequent energy monitoring, while high-speed mobility intensifies route maintenance from link breaks, further increasing overhead. Although AODV-C selects paths within localized areas, its neglect of node energy states reduces adaptability at high speeds, resulting in higher overhead than AODV-E. SE-AODV achieves the lowest overhead by reducing baseline costs through constrained flooding areas and enhancing path stability via energy-based selection. It reduces overhead by approximately 60.69% versus AODV, and by 53.24% and 24.46% versus AODV-C and AODV-E respectively, demonstrating superior adaptability in high-mobility scenarios.

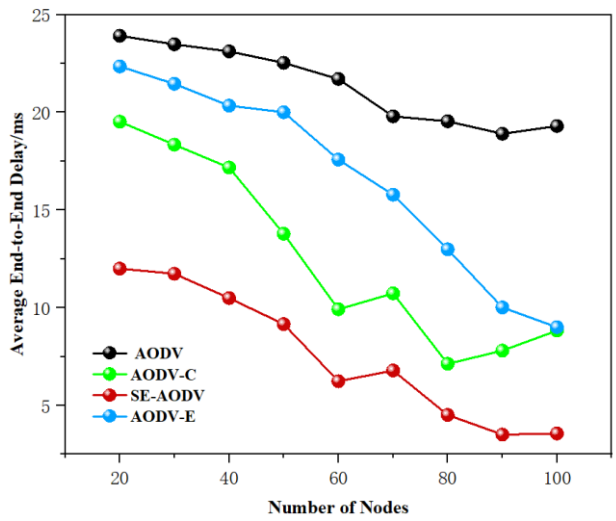


Figure 11 The impact of number of nodes on average end-to-end delay

Figures 11-13 present simulation results for average end-to-end delay, packet delivery ratio, and routing control overhead under varying node counts. Figure 11 shows that at 20 nodes, all four protocols exhibit relatively high delay due to larger internode distances causing unstable data forwarding/reception. As node count increases to sufficient density, network paths shorten with fewer hops between source and destination, reducing delay. Although AODV-E prioritizes high-energy nodes, path redundancy intensifies with growing node count, resulting in higher delay than AODV-C and SE-AODV. AODV-C restricts route request scope to reduce redundant probing, demonstrating effective delay control. SE-AODV improves broadcast route requests and minimum-hop selection, reducing delay by approximately 56.85% versus traditional AODV in dense networks, and by 25.83% and 51.74% versus AODV-C and AODV-E respectively.

Figure 12 indicates rising packet delivery ratios with increasing node density. This occurs because denser networks provide more stable transmission paths, gradually improving delivery. SE-AODV performs optimally, while AODV shows the lowest delivery. AODV-C's neglect of energy factors leads to selecting fragile minimum-hop paths, causing slight delivery degradation at higher node counts. AODV-E avoids low-energy nodes to reduce link failures but suffers timeout risks from detours, maintaining marginally higher delivery than AODV. SE-AODV selects energy-sufficient stable links, achieving superior delivery at scale—improving by approximately 88.07% over AODV, 40.22% over AODV-C, and 78.19% over AODV-E.

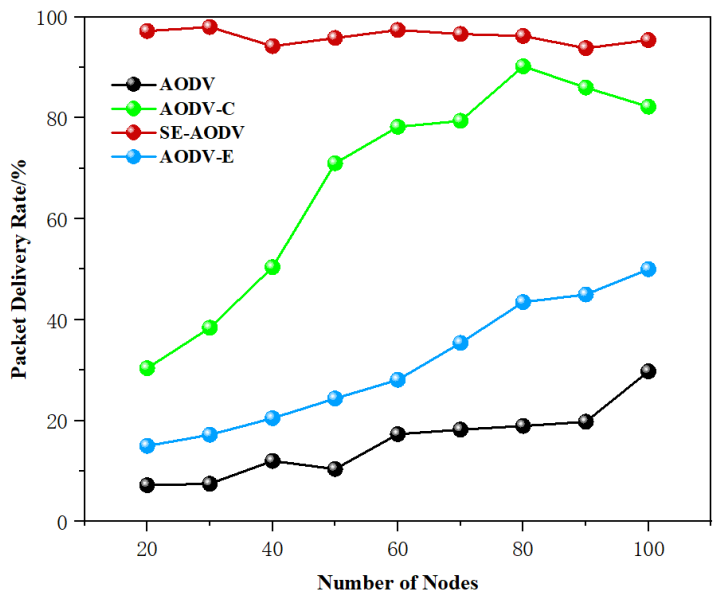


Figure 12The impact of number of nodes on packet delivery rate

| IJMER | ISSN: 2249–6645 | | Vol. 15 | Iss. 6 | www.ijmer.com

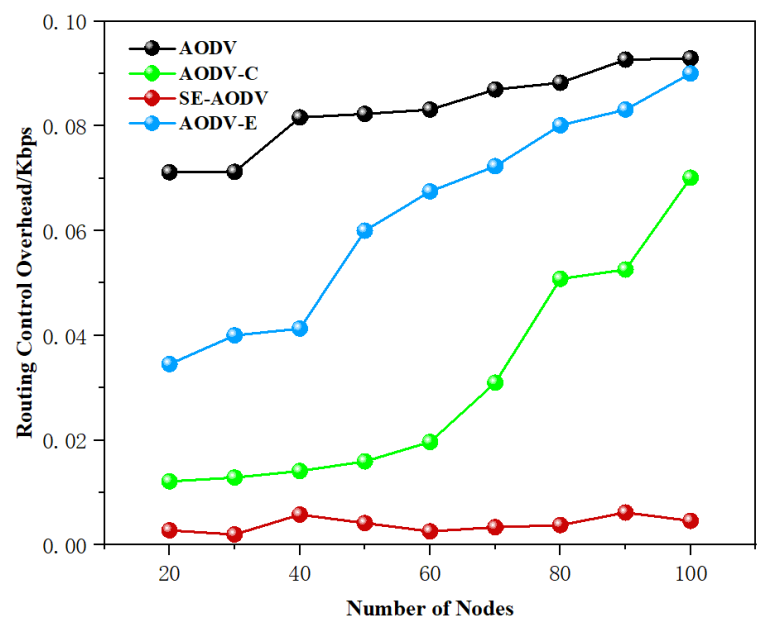


Figure 13 The impact of number of nodes on routing control overhead

Figure 13 demonstrates routing control overhead variation with node count. Increasing nodes necessitate more route maintenance, elevating overhead. AODV-E's energy monitoring and frequent rerouting incur substantial overhead second only to AODV. AODV-C significantly reduces requests through flood restriction but maintains higher overhead than SE-AODV. SE-AODV maintains the lowest and most stable overhead by selecting stable links while minimizing redundancy, reducing control overhead by approximately 95.58% versus AODV, and 76.15% and 89.4% versus AODV-C and AODV-E respectively.

VI. Conclusion

This paper addresses the problem of link breakage in MANET networks caused by node energy depletion or nodes moving out of the communication range, and proposes the SE-AODV protocol algorithm. An optimal search area is designed based on the path hop counts and positions of the nodes at the breakage point and their upstream nodes. Then, nodes with the optimal energy are selected for data forwarding according to the ratio of remaining energy consumption. Simulation experiments with AODV, AODV-C, and AODV-E show that in terms of three indicators, namely the average end-to-end delay, the packet delivery ratio of different packet groups, and the routing control overhead, the proposed algorithm significantly outperforms other protocols under different packet sending rates of nodes, different moving speeds of nodes, and different numbers of nodes.

Acknowledgements

This work was supported by the Natural Science Foundation of Hunan University of Science and Technology Transfer Project (No.K1A169).

References

- [1]. ZAFAR W, KHAN B M. Flying Ad-hoc network: Technological and social implications[J]. IEEE Technology and Society Magazine. 2016;35(2):67-74.
- [2]. LU Han, XIA Weiwei, HE Guangyue. An Improved DSDV Routing Algorithm For BLE Audio[J]. Mobile Communications. 2023;47(10):71-77+92.
- Fahad Ahmad Al Zahrani. On Modeling Optimizations and Enhancing Routing Protocols for Wireless MultiloopNetworks[J]. IEEE Access.2020: 68953-68973.
- [4]. Kim N, Na W, Cho S. Dual-Channel-Based Mobile Ad Hoc Network Routing Technique for Indoor Disaster Environment[J]. IEEE Access.2020;8126713-126724.
- [5]. Deepak S, Nisha S, Kumar S M, et al. Analysis and comparison of ant colony optimization algorithm with DSDV, AODV, and AOMDV based on shortest path in MANET[J]. Journal of Information and Optimization Sciences. 2020;41(2):621-632.
- [6]. JAIN R, KASHYAP I. An QoS aware link defined OLSR(LD-OSLR) Routing Protocol for MANETS[J]. Wireless Personal Communications. 2019;4(6):1-14.
- [7]. LADAS A, PAVLATOS N, WEERASINGHE N, et al. Multipath routing approach to enhance resiliency and scalability in ad-hoc networks[C]. IEEE International Conference on Communications (ICC). 2016;1-6.

- [8]. Khandekar A V, Gupta P. Machine Learning-Based Hybrid SSO-MA with Optimized Secure Link State Routing Protocol in Manet[J]. China Communications. 2025;22(03):164-180
- [9]. Usha M, Ramakrishnan B. A robust architecture of the OLSR protocol for channel utilization and optimized transmission using minimal multi point relay selection in VANET[J]. Wireless Personal Communications. 2019;109(1):271-295.
- [10]. Zhang Degan, Cui Yuya, Zhang Ting. New quantum-genetic based OLSR protocol(QG-OLSR) for mobile Ad hoc network[J]. Applied Soft Computing. 2019;80(8):285-296.
- YI Changhua, JIANG Peng, LU Qian, ZHOU Liang. Research on DSR-based routing optimization of ship Ad Hoc networks[J]. [11]. Modern Electronics Technique. 2023;46(8):106-110.
- [12]. Ankita A, Mahamune, and M.M.Chandane. Trust-based co-operative routing for secure communication in mobile ad hoc networks[J]. Digital Communications and Networks. 2024;10(4):1079-1087.
- HE Dong, Yu Jiyan. Speed Aware Routing Algorithm for Multi-Missile Network Based on AODV[J]. Journal of Ordnance [13]. Equipment Engineering. 2019;40(5): 137-141.
- [14]. S. T, B. A, N. S D. Bio-inspired deep residual neural network learning model for QoS routing enhancement in mobile ad-hoc networks[J]. Wireless Networks. 2023;29(8):3541-3565.
- V. B S, P. S. Detection and Isolation of Selfish Nodes in MANET Using Collaborative Contact-Based Watchdog with [15]. Chimp-AODV[J]. Wireless Personal Communications. 2022;128(2):1373-1390
- Priyanka P, Raghuraj S. Efficient Route Selection Scheme in MANET Using Enhanced AODV Protocol[J]. Wireless Personal Communications. 2021;123(1):959-974.
- [17]. Ejmaa AME, Subramaniam S, Zukarnain ZA, et al. Neighbor-based dynamic connectivity factor routing protocol for mobile ad hoc network[J]. IEEE Access. 2016;4(99):8053-8064.
- [18]. ZOU Xiuming. AODV routing protocol of greater energy and signal strength node first. Computer Engineering and Applications[J]. Computer Engineering & Applications, 2014;50(17):86-89.
- [19]. R. Shanmugavalli, M. Krishnaveni, T. Dhivyaprabha and P. Subashini. Energy Aware Routing Mechanism Using AODV Protocol For Low Energy Consumption in WSN[C]. IEEE 5th International Conference on Cybernetics, Cognition and Machine Learning Applications (ICCCMLA). 2023;242-247.
- [20]. Chen KS, Li HK, Ruan YL, Wang SH. Improved AODV routing protocol based on local neighbor nodes and link weights[J]. Journal of Software. 2021;32(4):1186-1200.
- [21]. Wang QW, Qi Q, Cheng W, Li D. Node degree estimation and static game forwarding strategy based routing protocol for ad hoc networks[J]. Journal of Software. 2020;31(6):1802-1816.
- Chen Shuwang, Song Shuli, Song Tongtong, et al. Improve AODV routing protocol based on energy balance and congestion[J]. [22]. Science Technology and Engineering. 2020;20(12):4798-4802.
- [23]. N. G. Razafindrobelina, R. Anggoro and A. M. Shiddiqi. The development of a routing protocol based on reverse-AODV by considering an energy threshold in VANET[C]. IEEE Int. IoT Electron. Mechatronics Conf. (IEMTRONICS). 2021;1-7.
- [24]. A. K. Dogra. Q-AODV: A flood control ad-hoc on demand distance vector routing protocol[C]. IEEE 1st Int. Conf. Secure Cyber Comput. Commun. (ICSCCC). 2018;294-299.
- [25]. B. Ardianto, H. S. D. Nurcahyo et al. Performance Comparison of AODV AODV-ETX and Modified AODV-ETX in VANET using NS3[C]. IEEE International Conference on Cybernetics and Computational Intelligence (Cyber-neticsCom). 2022.
- E. Setijadi, I. K. E. Purnama and M. H. Pumomo. Performance comparative of AODV, AOMDV and DSDV routing protocols in MANET using NS2[C]. Proc. Int. Seminar Appl. Technol. Inf. Commun. 2018;286-289.
- [27]. B. Patel and D. R. Patel. Study of Denial of Service Attack On AODV Routing Protocol in Mobile Ad-hoc Network[C]. 2023 International Conference on Artificial Intelligence and Smart Communication (AISC). 2023;66-77
- [28]. Tang Mingtian, Lin Xiaola, Maurizio P. The repetitive turn model for adaptive routing[J]. IEEE Transactions on computers. 2017:66(1):138-146.
- B. R. Hanji and R. Shettar. Enhanced AODV Multipath routing based on node location[C]. International Conference on [29]. Computation System and Information Technology for Sustainable Solutions (CSITSS). 2016;158-162.
- [30]. Zhang, D.-G., Chen, L., Zhang, J., Chen, J., Zhang, T., Tang, Y.-M., Qiu, J.-N. A multi-path routing protocol based on link lifetime and energy consumption prediction for mobile edge computing[J]. IEEE Access. 2020;8:69058-69071.
- [31]. Ramesh and G. Seshikala. Link Aware Multipath Routing to Defend Against Black Hole Attacks for MANETs[C]. International Conference on Intelligent Technologies (CONIT). 2023;1-6.

| IJMER | ISSN: 2249–6645 |